Temperature and doping dependence of electron spin relaxation in GaSb

2009 Semicond. Sci. Technol. 24 025018

(http://iopscience.iop.org/0268-1242/24/2/025018)

Semicond. Sci. Technol. **24** (2009) 025018 (6pp) doi:10.1088/0268-1242/24/2/025018

Temperature and doping dependence of electron spin relaxation in GaSb

C Hautmann[1], F Jaworeck[1], K Kashani-Shirazi[2], M-C Amann[2] and M Betz[1]

[1] Physik-Department E11, Technische Universität München, 85748 Garching, Germany
[2] Walter Schottky-Institut and Physik-Department E26, Technische Universität München, 85748 Garching, Germany

E-mail: mbetz@ph.tum.de

Received 27 November 2008, in final form 2 December 2008
Published 20 January 2009
Online at stacks.iop.org/SST/24/025018

Abstract
Electron spin relaxation times in *n*-doped as well as in nominally undoped bulk GaSb are measured with time-resolved circular dichroism and Faraday rotation induced by 1.55 μm, 150 fs pulses. Degenerately *n*-doped samples are characterized by ultrashort relaxation times of $\sim$2 ps. In contrast, we find much larger time constants and a strong temperature dependence of the spin relaxation time in moderately *n*-doped and undoped GaSb. The longest spin relaxation time is found to be $\sim$30 ps for an undoped sample at temperatures below $T = 50$ K. Many aspects of the results can be attributed to the large spin–orbit coupling in GaSb, consistent with the D'yakonov–Perel' theory of spin relaxation. In addition, magneto-optical measurements reveal an effective electronic Landé factor of $|g^*| = 9 \pm 1$.

1. Introduction

The enormous potential of spin-based devices has triggered intensive experimental and theoretical efforts on the physics of carrier spins in semiconductors [1]. While rapid progress has been achieved towards long-lived electron-spin polarizations [2, 3] and their transport properties over macroscopic distances [4], there are still important questions regarding the microscopic details of spin dynamics in semiconductors. As an example, strong spin–orbit (SO) interaction has been predicted [5] and shown [6] to induce a complex sub-picosecond dynamics of hole spins in GaAs. In most semiconductors, strong SO coupling is only relevant for holes because p-like states experience this coupling directly. In materials such as GaSb and InSb, however, the energy scale of the SO splitting is comparable or even larger than the bandgap energy and, therefore, also electrons are expected to experience strong SO coupling. In zinc-blende semiconductors, SO coupling lifts the degeneracy of the spin up and down electronic states. This can effectively be described in terms of a $\vec{\mathbf{k}}$-dependent magnetic field that induces a precession of the carrier spin and, thereby, implies a decay of the total spin polarization. In addition, SO coupling leads to a momentum-dependent mixing of spin and orbital momentum eigenstates so that scattering processes can change not only orbital angular momentum but also the spin state. GaSb, in particular, has recently gained considerable attention because its bandgap energy is favourable for device applications at 1.55 μm. While the electron spin relaxation time in GaSb has been predicted to strongly depend on both temperature and doping [7, 8], an experimental investigation of these trends is still missing.

In this paper, we analyse electron spin relaxation in bulk GaSb with ultrafast optical orientation methods. In particular, nominally undoped samples are compared to both degenerately and non-degenerately *n*-doped specimens. The measurements reveal a picosecond decay of the electron spin polarization. Model calculations mainly based on the D'yakonov–Perel' (DP) spin relaxation mechanism explain many aspects of the temperature and doping dependence of the spin relaxation time. For low temperatures, however, the observed spin lifetime is drastically shorter than the sub-nanosecond or even nanosecond timescales predicted by both a non-degenerate DP model [8] and more sophisticated simulations [7]. Finally, we analyse the coherent precession of electron spins in an external magnetic field and deduce a *g* factor of $|g^*| = 9 \pm 1$ for electrons in bulk GaSb.

2. Samples and experimental setup

The 1 μm thick bulk GaSb samples are grown by molecular beam epitaxy on intrinsic GaAs substrates. To reduce the density of dislocations related to the lattice mismatch between GaAs and GaSb, a GaSb/AlSb superlattice is grown prior to deposition of bulk GaSb. Measurements of the carrier mobilities (see below) point towards electronic transport properties close to the values reported for epitaxial GaSb. *n*-conducting layers with carrier concentrations of $n = 1.2 \times 10^{17}$ cm^{-3} and $n = 1.5 \times 10^{18}$ cm^{-3} are grown by doping with Te. The samples are mounted in an optical microscope cryostat operated between $T = 5$ K and room temperature. The experimental set-up relies on an amplified modelocked Er:fiber laser (Toptica FFS) yielding 1.55 μm, 150 fs pulses with a repetition rate of 80 MHz and an average power of 250 mW. In particular, the central photon energy of 0.8 eV is in the vicinity of the bandgap energy of GaSb for all temperatures and doping levels of this study. The major fraction of the pulse train serves as a circularly polarized pump pulse and excites a partially spin-polarized electron distribution [9] according to the interband optical selection rules for heavy hole and light hole transitions. Note that the hole spin is expected to decay on a timescale comparable or shorter than the pulse duration [6] so that we restrict the consideration to electron spins. The transient spin population is detected with two complementary pump–probe techniques in transmission geometry: the first relies on the fact that spin-polarized electrons generate different optical bleaching signals for probe light co- or counter-circularly polarized with respect to the excitation pulse. As a result, any circular dichroism reflects the transient electron spin polarization. Alternatively, the spin dynamics is also accessible in a Faraday rotation type experiment, i.e. spin-polarized carriers effectively yield a polarization rotation of a linearly polarized probe beam which is measured with a polarization bridge.

3. Results: ultrafast optical orientation

First, we analyse electron spin relaxation in an *n*-doped GaSb layer with a carrier concentration of $n = 1.2 \times 10^{17}$ cm^{-3}. The filled (open) circles in figure 1(*a*) show the transmission changes obtained for σ^+ (σ^-) polarized probe light as a function of the delay time elapsed since the excitation with a σ^+ polarized pump beam generated an electron–hole density of $n \sim 1 \times 10^{16}$ cm^{-3} at a temperature of $T = 100$ K. The results are indicative of a pronounced circular dichroism. The difference of the two transmission changes divided by their sum (squares in figure 1(*b*)), which is proportional to the spin polarization [10], decays with a time constant of 10 ps. The triangles in figure 1(*b*) display the transient Faraday rotation observed for the same excitation conditions; the data corroborate the above time constant and its interpretation as an electron spin relaxation time. Studies as displayed in figure 1 are performed for a wide range of temperatures, doping levels and pump intensities. Figure 2(*a*) displays the temperature-dependent electron spin relaxation time extracted from transient circular dichroism and/or Faraday rotation

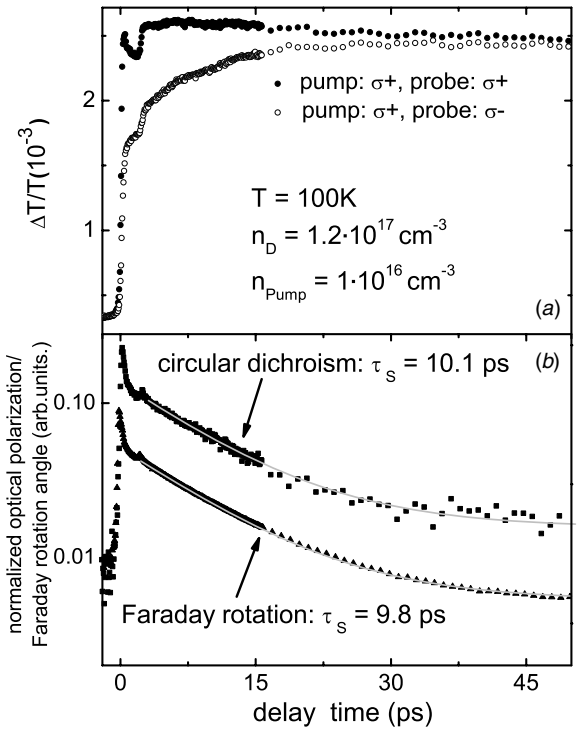

Figure 1. (*a*) Transient differential transmission of a 1 μm thick layer of GaSb with a doping level of $n = 1.2 \times 10^{17}$ cm^{-3}. Solid (open) circles: co-circular (counter-circular) optical polarization of 150 fs, 1.55 μm excitation and probe pulses. (*b*) Squares: normalized circular dichroism extracted from the data in panel (*a*). Triangles: transient Faraday rotation angles for the same experimental conditions. The solid grey lines represent exponential fits to the experimental data.

measurements on the $n = 1.2 \times 10^{17}$ cm^{-3} sample. It is seen to slowly decay from 14 ps at low temperatures to 4 ps at room temperature. We note that the reduction of the bandgap energy for elevated temperatures effectively yields an increase of the density of pump-generated electron–hole pairs with temperature. However, as we will detail below, the present measurements take place in the weak excitation limit where the spin relaxation time does not significantly depend on the carrier density. In addition to these optical measurements, we also analyse the carrier mobility of the GaSb layer with Hall measurements in a van der Pauw geometry and obtain values of $\mu = 6400$ cm^2 Vs^{-1}, $n = 1.8 \times 10^{17}$ cm^{-3} ($\mu = 3500$ cm^2 Vs^{-1}, $n = 1.2 \times 10^{17}$ cm^{-3}) at $T = 77$ K (room temperature). The rather counterintuitive temperature dependence of the carrier concentration is a result of DX centres in *n*-GaSb which act as deep acceptors at room temperature while they behave as shallow donors at low temperatures [11]. To facilitate the understanding of the observed temperature dependence of the spin relaxation time, we perform model calculations based on the general expectations of the dominant spin relaxation mechanisms before comparing the results to more elaborate simulations. For high mobility samples the electron spin relaxation is predicted to be dominated by the DP process [8]. This mechanism is related to the energetic splitting of spin-up and

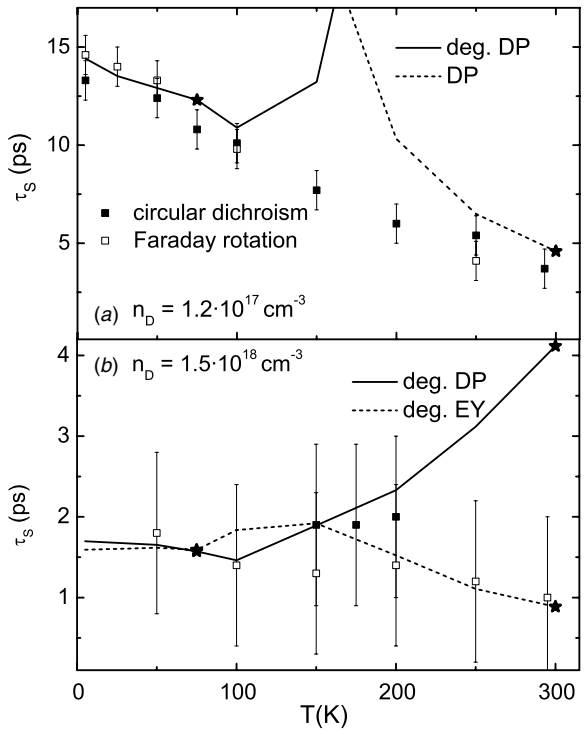

Figure 2. Spin relaxation times in GaSb extracted from transient circular dichroism (solid squares) and/or Faraday rotation measurements (open squares) for various temperatures. (*a*) Results for an *n*-doped specimen with $n = 1.2 \times 10^{17}$ cm^{-3}. (*b*) Corresponding spin relaxation times for a sample with $n = 1.5 \times 10^{18}$ cm^{-3}. The solid and dashed lines represent theoretical expectations for the DP and EY scattering mechanisms as detailed in the main text. (The stars indicate points of measured Hall data.)

spin-down electrons for a specific state $\mathbf{k}$ and is predicted to yield a spin-relaxation rate $\frac{1}{\tau_s}$ of [12, 13]

$$\frac{1}{\tau_s} = q\alpha^2 \frac{E_{\mathbf{k}}^3}{\hbar^2 E_g} \tau_p(E_{\mathbf{k}}). \tag{1}$$

Here, $\tau_p(E_{\mathbf{k}})$ denotes the momentum relaxation time of an electron with a kinetic energy of $E_{\mathbf{k}}$ and $\alpha = \frac{4\gamma}{\sqrt{(3-\gamma)}} m_e$ (with $\gamma = \frac{\Delta}{\Delta + E_g}$ and with the electron effective mass m_e in units of the free electron mass) characterizes the strength of the SO interaction for a semiconductor with bandgap energy E_g and split-off energy Δ. q is a dimensionless factor and depends on the dominant momentum scattering mechanism. For low temperatures, a doping density of $n \sim 10^{17}$ cm^{-3} implies a degenerately occupied conduction band and the average DP scattering time is predicted to be

$$\frac{1}{\tau_s} = q\alpha^2 \frac{(E_F)^3}{\hbar^2 E_g} \tau_p \tag{2}$$

for a Fermi energy E_F. The solid line in figure 2(*a*) shows the resulting spin relaxation time for a Fermi energy of $E_F = 30$ meV (as calculated in the Nilsson approximation [14] for $T = 77$ K), the actual electron mobility at $T = 77$ K and its expected temperature dependence [15]. Note that we use $q = 3.2$ in equation (1) to obtain agreement with the low temperature spin relaxation time of the experiment. Similar values of q have been reported, e.g., for deformation potential scattering in non-degenerately doped semiconductors. In contrast, ionized impurity scattering in a degenerately doped material is predicted to be characterized by $q \approx 0.05$ [12], i.e. one expects a ∼50 times larger spin relaxation time. This discrepancy might in part be related to the sample being a thin layer with dislocations at the film-substrate interface. As an example, a recent analysis of spin relaxation in InSb [16] and InAs [17] thin films suggests a dislocation mediated increase of the spin relaxation rate. In addition, carrier accumulation or depletion at surfaces and interfaces likely leads to deviations of the measured electron mobility from the actual bulk transport properties [18]. For temperatures approaching ambient values and $n = 1.2 \times 10^{17}$ cm^{-3}, one expects the electron distribution in the conduction band to be close to the Boltzmann limit. For such a non-degenerate situation, the DP theory predicts an average spin relaxation rate of

$$\frac{1}{\tau_s} = q\alpha^2 \frac{(kT)^3}{\hbar^2 E_g} \tau_p. \tag{3}$$

The temperature dependence of the spin relaxation time according to this equation and the assumption of $q = 20$ is plotted as a dashed line in figure 2(*a*). Again, we note that we have to choose an unexpectedly large value of q in order to reproduce the ultrashort spin relaxation time of 4 ps at room temperature. As seen in figure 2(*a*), neither model reproduces the observed spin relaxation time for intermediate temperatures. In this case, a quantitative understanding of the electron spin relaxation would require a more sophisticated computation of the average momentum relaxation of a partially degenerate electron gas which is beyond the scope of the present consideration. It is also interesting to compare our findings to results of a recent simulation of the electron spin relaxation in moderately doped GaSb: Song and Kim [8] predict a room temperature spin lifetime of several ps as seen in the experiment. For low temperatures, however, their results indicate spin relaxation times of more than one ns. This discrepancy is likely related to their assumption of a non-degenerate carrier statistics which seems inappropriate for a $n \sim 10^{17}$ cm^{-3} doped sample at somewhat lower temperatures.

We now turn to the analysis of electron spin relaxation in a GaSb layer with a donor doping level of $n = 1.5 \times 10^{18}$ cm^{-3} where the electron distribution is expected to be degenerate up to room temperature. As depicted in figure 2(*b*), the ultrafast optical orientation measurements point towards spin lifetimes as short as 1–2 ps for all the temperatures of this study. Hall measurements reveal electron mobilities and carrier concentrations of $\mu = 2400$ cm^2 Vs^{-1}, $n = 1.7 \times 10^{18}$ cm^{-3} ($\mu = 1200$ cm^2 Vs^{-1}, $n = 1.5 \times 10^{18}$ cm^{-3}) at $T = 77$ K (room temperature). In this regime of intermediate mobilities both the DP mechanism and the Elliott–Yafet (EY) spin relaxation can limit the spin lifetime. The EY mechanism [19, 20] is related to scattering processes that simultaneously change spin and orbital angular momentum.

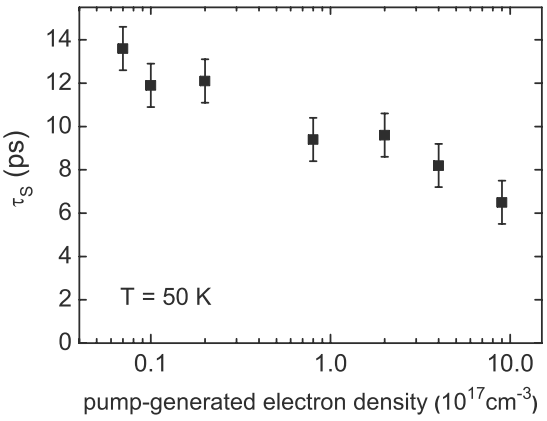

Figure 3. Spin relaxation times extracted from time-resolved circular dichroism measurements in the $n = 1.2 \times 10^{17}$ cm^{-3} GaSb sample for various excitation intensities and a lattice temperature of $T = 50$ K.

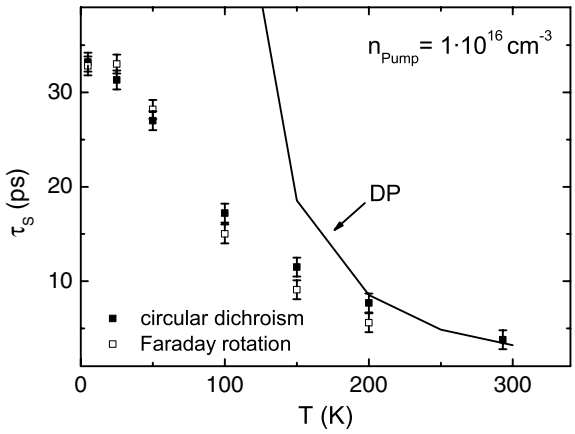

Figure 4. Spin relaxation times extracted from time-resolved circular dichroism and/or Faraday rotation measurements in a 1 μm thick, nominally undoped GaSb layer for various temperatures. The solid line shows the spin relaxation expected from the DP mechanism.

For a degenerately doped semiconductor, it is predicted to give rise to a scattering rate of [8, 21]

$$\frac{1}{\tau_s} = A\beta^2 \left(\frac{E_F}{E_g}\right)^2 \frac{1}{\tau_p}, \tag{4}$$

where $\beta = \frac{\gamma(1-\frac{\gamma}{2})}{(1-\frac{\gamma}{3})}$ (with $\gamma = \frac{\Delta}{\Delta+E_g}$) describes the strength of the SO induced mixing of the spin eigenstates and A depends on the dominant momentum relaxation mechanism. The solid line in figure 2(*b*) shows the result for the DP spin relaxation time computed from equation (2) with $E_F = 130$ meV and $q = 0.8$. While this theory agrees well with the observed low temperature spin relaxation time, the rather low mobility at room temperature would give rise to a DP spin lifetime of ∼4 ps. In contrast, the result for the EY mechanism with $A = 6$ yields low temperature scattering rates similar to the DP values but also reproduces the room temperature lifetime of the experiment. Taken together, it seems likely that both scattering mechanisms contribute to the comparatively fast spin relaxation. It is again instructive to compare the experimental results to more sophisticated simulations of the electron spin relaxation in GaSb. Lau *et al* [7] consider a dopant concentration of $n \approx 1.5 \times 10^{18}$ cm^{-3} and compute the electron spin relaxation in a nonperturbative nanostructure model. They predict the electron spin relaxation time to strongly increase from a value of ∼3 ps at room temperature to ∼300 ps at $T = 4$ K. Song and Kim [8] simulate on an even stronger temperature dependence with a low temperature electron spin relaxation time of several ns at cryogenic temperatures in marked contrast to the ∼2 ps found in the experiment (note: Song and Kim use a non-degenerate carrier statistics even for a doping level $n \sim 10^{18}$ cm^{-3}). As a result, these theoretical results clearly overestimate the electron spin lifetime at lower temperatures. We note that similar discrepancies between spin lifetimes predicted by DP models and experimental results at low temperatures are also found in InSb [16] and GaAs [7].

Electron spin relaxation is also analysed as a function of the density of the electron–hole gas generated by the pump pulse. Figure 3 displays the spin lifetime extracted from transient circular dichroism signals for pump-generated carrier densities 7×10^{15} cm$^{-3} \leqslant n_{\rm pump} \leqslant 1 \times 10^{18}$ cm^{-3} and a lattice temperature of $T = 50$ K. It decreases from 14 ps for photogenerated carrier densities well below the dopant density to ∼6 ps for strong excitation conditions. At first glance, this trend contradicts the interpretation as a DP dominated spin relaxation above. In particular, stronger electron–electron scattering might be expected to decrease the spin relaxation rate in the case of DP-type relaxation [22]. However, the excitation of a large density of electron–hole pairs implies the occupation of energetically higher conduction band states so that the Fermi energy for a doping level of ∼10^{17}cm^{-3} at low temperatures underestimates the spin relaxation rates. We note that the data in the figures 1 and 2 have been obtained with excitation intensities comparable to the lowest value used in figure 3.

Now we compare the above results for *n*-doped GaSb layers to a nominally undoped sample. Hall measurements indicate a remaining p-type conduction, a density of impurities of $\sim 1 \times 10^{16}$ cm^{-3} and a room temperature hole mobility of ∼300 cm^2 Vs^{-1}. While the electron mobility is not directly accessible in this experiment, it is expected to be ∼9000 cm^2 Vs^{-1} [15, 23], i.e. larger than in moderately doped GaSb. Spin relaxation times extracted from transient circular dichroism and/or Faraday rotation for various temperatures are shown in figure 4. Below 50 K, we find spin lifetimes of ∼30 ps. This value is twice as long as observed for $n = 1.2 \times 10^{17}$ cm^{-3} specimen. For higher temperatures, the spin lifetime strongly decreases towards a room temperature level of 4 ps, i.e. comparable to the time constant seen in the moderately *n*-doped specimen (cf figure 2(*a*)). We note that this time constant is a factor of ∼4 larger than in undoped GaSb quantum wells where quantum confinement leads to an enhancement of the DP scattering rate [26]. The solid line in figure 4 shows the result for the DP scattering time according to equation (2). As already seen above, we have to use an unexpectedly large value of $q = 10$ in equation (2) to reproduce the ultrashort spin lifetime at room temperature.

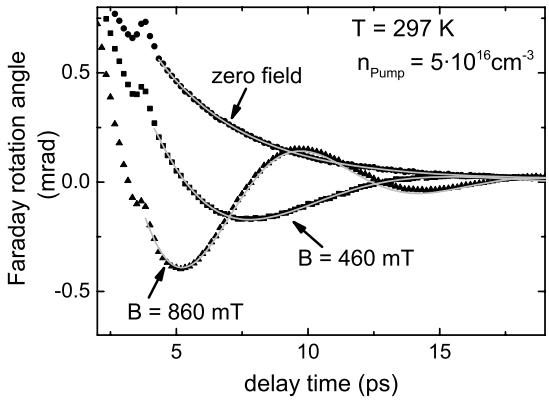

Figure 5. Transient Faraday rotation angles after photogeneration of a carrier density of $n_{\mathrm{pump}} = 5 \times 10^{16}$ cm^{-3} with a circularly polarized pump pulse for magnetic fields B of zero, 460 mT and 860 mT. The grey lines correspond to single exponential decays ($B = 0$ mT) and exponentially damped sinusoids ($B = 460$ mT, $B = 860$ mT).

In addition, the DP model predicts a tremendous increase of the spin lifetime for low temperatures which is not found in the experiment. This deviation might be related to the rather complex structure of impurities acting as acceptors in nominally undoped GaSb [27] which apparently are not well described by the assumption of a pure DP mechanism. We note that the residual p-conductivity potentially also limits the electron spin lifetime at low temperatures. In particular, the simulation of Song and Kim [8] predicts spin relaxation times of ∼250 ps for slightly p-doped GaSb which they attribute to electron–hole spin-exchange via the Bir–Aronov–Pikus mechanism [28].

4. Results: ultrafast magneto-optics

Finally, we want to address potential coherent manipulation of electron spins in GaSb. To this end, we study the nominally undoped GaSb specimen in a room temperature magneto-optical set-up. In particular, in-plane magnetic fields of up to ∼1 T are applied in a Voigt geometry and we detect transient Faraday rotation angles after ultrafast photoexcitation with a circularly polarized 1.55 μm, 150 fs pulse. Figure 5 shows the results for a photogenerated carrier density of $n_{\mathrm{pump}} = 5 \times 10^{16}$ cm^{-3}. The curve without an applied magnetic field corresponds to the results discussed above. The electron spins injected by a circularly polarized normal incidence pump beam are polarized normal to the sample plane. Under the influence of an external magnetic field B these spins undergo Larmor precession about the field axis. While decaying with the spin lifetime, the optical polarization is therefore expected to oscillate with an angular frequency of $\frac{g^*\mu_B B}{\hbar}$ with the effective Lande factor g^* and the Bohr magneton μ_B. The results for $B = 460$ mT and $B = 860$ mT are shown in figure 5. In particular, we find a strongly damped oscillatory transient for both values of the external field. Fits of the results with applied magnetic field with exponentially damped sinusoids reveal a spin lifetime of ∼4 ps which corroborates the observations above. We note that the decay times in figure 5 are found to increase from 3.5 ps at B = 0 to 4.5 ps at B = 860 mT. This finding could result from slightly different decay times T_1 and T_2 for longitudinal and transverse spin order, respectively. These two times should in principle be identical for a bulk semiconductor of cubic symmetry [7], but, e.g., a built-in field at the surface or substrate interface could induce a structural inversion asymmetry and thereby lift the symmetry requirement $T_1 = T_2$. Alternatively, the spin precession in an external magnetic field has been reported to have an influence similar to averaging by random scattering [29]. In particular, a spin relaxation time that increases with the magnetic field is therefore consistent with a suppression of DP-type scattering by the orbital motion induced by the field. For the Lande g^* factor we extract a value $|g^*| = 9 \pm 1$. Note that our measurement method is not sensitive to the sign of the g^*-factor which, however, is known to be negative in GaSb. This is in agreement to the values of $|g^*| = 9.3$ and $g^* = -7.8 \pm 0.8$ found by Hermann *et al* [30] and Reine *et al* [31], respectively, while it is slightly higher than the theoretical prediction of $g^* = -6.7$ [32]. We did not perform a more detailed study of the magneto-optical properties of GaSb for different temperatures and doping levels because the present set-up only allows for room temperature measurements and, thus, all the samples are expected to exhibit a strongly damped Larmor precession.

5. Conclusion

In conclusion, we have analysed electron spin dynamics in GaSb with ultrafast optical orientation methods. In particular, GaSb serves as a model system for strong spin–orbit coupling. We find the spin relaxation time not to exceed ∼35 ps even for low temperatures of $T = 5$ K and undoped specimens. A further significant reduction of the spin lifetime to values as low as a few ps is observed for both elevated temperatures and donor doping levels. Many of these trends directly result from the large SO coupling in GaSb and are consistent with the DP theory of spin relaxation although such theories tend to predict larger low-temperature spin lifetimes than experimentally observed. In addition, coherent electron spin precession in an external magnetic field is analysed with time-resolved Faraday rotation. The observed Larmor precession points towards a Lande factor of $|g^*| = 9 \pm 1$ while it is strongly damped due to the limited spin lifetime in GaSb.

Acknowledgments

We acknowledge valuable discussions with M S Brandt, S T B Gönnenwein, C Ruppert and M Wesseli. This work has been supported by the Deutsche Forschungsgemeinschaft in the framework of the Sonderforschungsbereich SFB631.

References

[1] Awschalom D D, Loss D and Samarth N 2002 *Semiconductor Spintronics and Quantum Computation* (Berlin: Springer)
[2] Kikkawa J M and Awschalom D D 2000 *Science* **287** 473
[3] Kroutvar M, Ducommun Y, Heiss D, Bichler M, Schuh D, Abstreiter G and Finley J J 2004 *Nature* **432** 81

[4] Kotissek P, Bailleul M, Sperl M, Spitzer A, Schuh D, Wegscheider W, Back C H and Bayreuther G 2007 *Nature Phys.* **3** 872
[5] Krauß M, Aeschlimann M and Schneider H C 2008 *Phys. Rev. Lett.* **100** 256601
[6] Hilton D J and Tang C L 2002 *Phys. Rev. Lett.* **89** 146601
[7] Lau W H, Olesberg J T and Flatté M E 2001 *Phys. Rev.* B **64** 161301
[8] Song P H and Kim K W 2002 *Phys. Rev.* B **66** 035207
[9] D'yakonov M I and Perel' V I 1971 *Sov. Phys.—JETP* **33** 1053
[10] Boggess T F, Olesberg J T, Yu C, Flatté M E and Lau W H 2000 *Appl. Phys. Lett.* **77** 1333
[11] Poole I 1990 *Appl. Phys. Lett.* **57** 1645
[12] D'yakonov M I and Perel' V I 1972 *Sov. Phys. Solid State* **13** 3023
[13] Pikus G E and Titkov A N 1984 *Optical Orientation* ed F Meier and B P Zakharchenya (Amsterdam: North-Holland)
[14] Nilsson N G 1973 *Phys. Status Solidi.* a **19** K75
[15] Baraldi A, Colonna F, Ghezzi C, Magnanini R, Parisini A, Tarricone L, Bosacchi A and Franchi S 1996 *Semicond. Sci. Technol.* **11** 1656
[16] Litvinenko K L, Nikzad L, Allam J, Murdin B N, Pidgeon C R, Harris J J, Zhang T and Cohen L F 2007 *J. Appl. Phys.* **101** 083105
[17] Litvinenko K L, Murdin B N, Allam J, Pidgeon C R, Zhang T, Harris J J, Cohen L F, Eustace D A and McComb D W 2006 *Phys. Rev.* B **74** 075331
[18] Petritz R L 1958 *Phys. Rev.* **110** 1254
[19] Elliott R J 1954 *Phys. Rev.* **96** 266
[20] Yafet Y 1963 *Solid State Physics* vol 14, ed F Seitz and D Turnbull (New York: Academic)
[21] Murdin B N *et al* 2005 *Phys. Rev.* B **72** 085346
[22] Glazov M M and Ivchenko E L 2004 *JETP* **99** 1279
[23] Chin V W 1995 *Solid State Electron.* **38** 59
[24] Kikkawa J M and Awschalom D D 1998 *Phys. Rev. Lett.* **80** 4313
[25] Dzhioev R I, Kavokin K V, Korenev V L, Lazarev M V, Meltser B Ya, Stepanova M N, Zakharchenya B P, Gammon D and Katzer D S 2002 *Phys. Rev.* B **66** 245204
[26] Hall K C, Leonard S W, van Driel H M, Kost A R, Selvig E and Chow D H 1999 *Appl. Phys. Lett.* **75** 3665
[27] Hu W 2004 *Phys. Lett.* A **332** 286
[28] Bir G L, Aronov A G and Pikus G E 1976 *Sov. Phys.—JETP* **42** 705
[29] Zutić I, Fabian J and Sarma S Das 2004 *Rev. Mod. Phys.* **76** 323
[30] Hermann C and Lampel G 1971 *Phys. Rev. Lett.* **27** 373
[31] Reine M, Aggarwal R L and Lax B 1972 *Phys. Rev.* B **5** 3033
[32] Higginbotham C W, Pollak F H and Cardona M 1968 *Proc. IX Int. Conf. on the Phys. Semiconductors* **1** 57